Astron. Astrophys. 265, 669–681 (1992)

ASTRONOMY AND ASTROPHYSICS

Circularly polarized spectroscopic observations of RS CVn systems*

J.-F. Donati[1,2], M. Semel[3], and D.E. Rees[4]

[1] Department of Astronomy, The University of Western Ontario, London, Ontario, N6A 3K7 Canada
[2] Département de Recherche Spatiale, Observatoire de Paris, Section de Meudon, F-92195 Meudon Principal Cédex, France
[3] Département d'Astronomie Solaire et Planétaire, Observatoire de Paris, Section de Meudon, F-92195 Meudon Principal Cédex, France
[4] CSIRO Division of Radiophysics, P.O. Box 76, Epping, NSW 2121, Australia

Received February 13, accepted March 20, 1992

Abstract. We applied the new technique of Zeeman–Doppler Imaging (measuring circularly polarized spectra to detect magnetic structures on rapidly rotating stars) on 9 active RS CVn binary systems. In 4 systems (HR 1099, σ^2 CrB, II Peg and UX Ari), we detected a magnetic field on the cool active component; in each of them, the corresponding Stokes V signature is found to vary with rotational phase. Moreover, on HR 1099, we have observational evidence that the magnetic structure varied significantly within a period of 1.3 yr. By contrast, magnetic field is repeatedly not detected on other stars, such as the hotter component of σ^2 CrB, although these are also chromospherically very active.

Our results suggest that the horizontal size scale of magnetic topologies may differ significantly among the observed stars. Large monopolar regions are likely present on those for which Zeeman signatures are detected; a more complex ordering of field lines with smaller monopolar regions and close bipolar groups may define the others. In σ^2 CrB for instance, the cooler and hotter components (though physically very similar except in effective temperature) have obvious and undetectable magnetic signatures respectively. We speculate that the size of monopolar magnetic regions may be related to the depth of the convection zone.

Key words: stars: magnetic fields – stars: binaries: spectroscopic – stars: late-type – line: profiles – polarization – stars: activity

1. Introduction

In a large number of late-type stars, activity indicators (e.g. photospheric spots discovered through photometric variability, lines of highly ionized elements providing evidence of chromospheres) are found to be essentially similar to those observed in the Sun, but with different strengths and horizontal scales. This common phenomenology is usually attributed to dynamo mechanisms, and primarily to their most important parameter, the magnetic field. In single stars of spectral type later than early G, the rotation rate is very slow, presumably due to some kind of magnetic braking (Gray 1988). By contrast, stars of the same spectral type associated in RS CVn binary systems [showing enhanced chromospheric activity (e.g. Strassmeier et al. 1988)] are usually rotating much faster due to the tidal coupling of components (Zahn 1977). Since activity (e.g. Strassmeier et al. 1990) and magnetic flux (Saar 1990) are observed to increase with rotation, RS CVn systems are optimal targets for studying stellar magnetic fields.

Before 1980, most attempts at detecting magnetic fields on cool stars followed the solar example and measured circular polarization in line profiles (e.g. Babcock 1958). Such measurements are sensitive to the line-of-sight component of the magnetic field vector (effective field) averaged over the observed region. However, since all active stars other than the Sun are angularly unresolved, only effective field values referring to the overall disc of the observed star could be derived with these first methods. The inconclusive results obtained by Brown & Landstreet (1981) and Borra et al. (1984) are presumably due to the complex magnetic topologies expected for this type of star. Not only can the large fraction of the stellar surface free of magnetic fields reduce greatly (by dilution) the average field, but also magnetic regions organized in many bipolar groups may cancel their mutual effect in the disc-integrated Stokes V profiles.

A new possible strategy was suggested by observations of Ap stars, in which strong fields generate nearly resolved splitting of unpolarized spectral lines (Preston 1971). Following Robinson (1980), most of the recent methods aim at modelling the *differential broadening* of absorption line profiles observed in unpolarized light. Such methods derive estimates for both the fraction of stellar surface covered with magnetic fields (filling factor f) and the mean field strength B inside the magnetic regions (see Saar 1990, 1991 for reviews). However, the Zeeman broadening of unpolarized profiles is very subtle and difficult to segregate from other sources of line broadenings like rotation or saturation. Therefore, errors as large as 50% are expected in both f and B if one is to consider all systematic perturbators (Saar 1991). Moreover, as stellar rotation increases [i.e. from $v \sin i \approx 8$ km s^{-1} (Saar

Send offprint requests to: J.-F. Donati (French address)
*Based on observations collected at the Canada-France Hawaii Telescope, Hawaii, and at the Anglo-Australian Telescope, Australia.

1988)], the magnetic broadening of unpolarized profiles is quickly drowned by rotation. These methods are thus totally inefficient for rapid rotators, although such stars are especially interesting since they are expected to be more magnetic (Saar 1990). But above all, filling factor and mean field strength measurements are not informative enough about the actual field *structure* for any accurate testing of the dynamo predictions on stars other than the Sun.

A breakthrough in this field may come with the method proposed by Semel (1989) called Zeeman–Doppler imaging (ZDI). It can be briefly described as Doppler imaging generalized to all Stokes parameters (and especially to circular polarization) and thus applies best to rapid rotators (i.e. $v \sin i > 20\ \mathrm{km\,s^{-1}}$) such as those associated in the very active RS CVn binary systems. For these stars, the Doppler effect separates in wavelength, in the disc-integrated polarized and unpolarized profiles, the contributions of stellar regions with different radical velocities. Such stars are then resolved spectroscopically in a direction perpendicular to the rotation axis and the line of sight so that each high resolution spectrum ($R > 40000$) can be regarded as a 1D image of the star. Viewing the star at different phases throughout the rotational cycle allows one, in principle, to recover the missing information and derive a 2D map of the star (Vogt 1988; Rice & Wehlau 1990; Piskunov et al. 1990; Brown et al. 1991).

ZDI has been applied to 9 very active RS CVn binary systems. In this paper, we first present the instrumentation and the data aquisition and reduction procedures with which our spectra are obtained. We then describe and comment on the spectropolarimetric observations made for each system, limiting ourselves to discussing on the statistical significance of any possible magnetic signatures.

2. Instrumentation and data processing

Only the major technical aspects will be reviewed here since both instrumentation and observing procedure have already been described (Semel et al. 1992; Donati et al. 1990a, b; Donati 1990).

With the present instrumentation, we only measure Stokes V and I spectra, since Stokes Q and U are much more difficult to obtain, being about one order of magnitude smaller. The expected typical total amplitude of a circular polarization profile associated with a strong (equivalent width $W \approx 200$ mÅ) and highly magnetic (effective Landé factor $g_{\mathrm{eff}} \approx 2$) line is of the order of 0.5% in units of the unpolarized continuum level. Thus, we aim at noise levels of about 0.1% or less. The instrumental device is a Zeeman polarimeter, i.e. a rotatable quarter-wave plate aligned with a beam-splitter to achieve a circular analysis of the stellar light. Switching the quarter-wave plate back and forth by an amount of 90° results in exchanging the left and right circular polarization states in all the following instrumentation.

Every stellar exposure is divided into two separate subexposures, each associated with a given position of the quarter-wave plate. Since both polarization states are recorded consecutively on the same CCD pixels, all pixel-to-pixel sensitivity variations in the spectra can be suppressed. Moreover, for each subexposure, both polarized states are measured simultaneously on the CCD detector, thereby compensating automatically for any temporal variation between the two subexposures (due to terrestrial or stellar rotation, stellar variability...). With such a procedure, all systematic errors are suppressed to first order in the derived Stokes V profiles (Semel et al. 1992).

The accuracy of these data aquisition and reduction procedures has been tested. With observations of the very bright Ap star ε UMa, we obtained Stokes V spectra with a relative noise level as low as 0.03% (Donati et al. 1990b). Solar light reflected from the moon was also measured for its very low amount of circular polarization in line profiles; even though its spectrum contains very sharp lines in which any crosstalk from Stokes I to V would be easily detectable, no indication of such an effect is observed up to a S/N value of 2000 (Donati et al. 1990a). We obtain spectra of the well known magnetic Ap star α^2 CVn and checked that the derived effective field (first moment of a Stokes V profile) agrees well with previously published values (Donati & Semel 1990). Finally, to be fully convinced that the circular polarization we observe in line profiles (whenever detected) is indeed due to magnetic fields, we checked that the amplitude of Zeeman signatures is larger for lines with higher magnetic sensitivities (see for instance Fig. 1).

To obtain such high S/N spectra in about 1% of a stellar rotation cycle, a 4 m class telescope is needed, even for the brightest of the very active RS CVn systems. Two different telescopes and instruments are presently involved in collecting the spectropolarimetric data. At the Anglo-Australian Telescope (AAT), the Cassegrain spectrograph of the Royal Greenwich Observatory (RGO) is used with an aberration free beam-splitter made of calcite block combinations (Semel 1987). At the Canada-France-Hawaii Telescope (CFHT), we feed the Coudé Spectrograph through a Bowen–Walraven image slicer and a fiber link from the polarimetric device mounted at the Cassegrain focus (see Semel et al. 1992 for details). With these spectrographs, the wavelength domain observed is centred at 5500 Å, spans a few tens of Å, and includes 3 nearly identical Fe I lines highly sensitive to magnetic fields. At the AAT, we use the RGO spectrograph with the 1200 J grating in second order and blaze-to-collimator

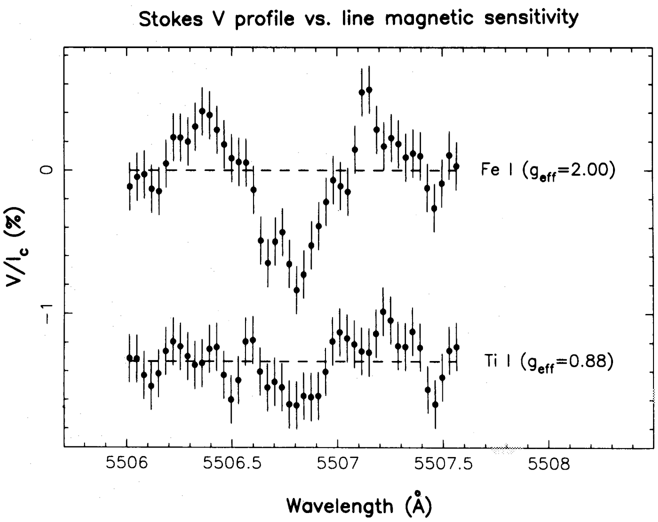

Fig. 1. Stokes V profiles of II Peg (at phase 0.479), for the $g_{\mathrm{eff}} = 2.00$ Fe I line at 5506.78 Å (upper curve), and for the $g_{\mathrm{eff}} \approx 0.88$ blend of two Ti I lines at 5514.35 and 5514.54 Å (lower curve). Larger distortions are seen in the Stokes V profile of the line with higher magnetic sensitivity, confirming the magnetic origin of this signature (note that the wavelength axis refers only to the Fe I line). As in all following graphs, the data points (filled circles) are plotted with a $\pm\sigma$ error bar

Table 1. Journal of spectroscopic observations

System	Site	Rot. phase	Date	JD (2 440 000 +)	Exp. time (min)	S/N (pxl^{-1})
HR 1099	AAT	0.488	1989 Aug. 17	7756.213	40	430
	AAT	0.511	1989 Aug. 17	7756.276	40	590
	AAT	0.522	1989 Aug. 17	7756.307	40	890
	AAT	0.530	1989 Aug. 17	7756.330	20	660
	AAT	0.829	1989 Aug. 18	7757.180	40	470
	AAT	0.840	1989 Aug. 18	7757.210	40	460
	AAT	0.850	1989 Aug. 18	7757.239	40	530
	AAT	0.861	1989 Aug. 18	7757.269	40	540
	AAT	0.871	1989 Aug. 18	7757.299	40	550
	AAT	0.879	1989 Aug. 18	7757.321	20	480
	CFHT	0.074	1990 Sep. 06	8140.970	40	870
	CFHT	0.085	1990 Sep. 06	8141.002	40	800
	CFHT	0.097	1990 Sep. 06	8141.035	40	820
	CFHT	0.107	1990 Sep. 06	8141.064	40	820
	CFHT	0.447	1990 Sep. 07	8142.027	40	920
	CFHT	0.457	1990 Sep. 07	8142.057	40	860
	CFHT	0.468	1990 Sep. 07	8142.087	40	900
	CFHT	0.479	1990 Sep. 07	8142.118	40	830
	CFHT	0.793	1990 Sep. 08	8143.009	40	960
	CFHT	0.803	1990 Sep. 08	8143.038	40	940
	CFHT	0.813	1990 Sep. 08	8143.066	40	1020
	CFHT	0.823	1990 Sep. 08	8143.094	40	900
	CFHT	0.136	1990 Sep. 09	8143.983	40	850
	CFHT	0.146	1990 Sep. 09	8144.011	40	820
	CFHT	0.161	1990 Sep. 09	8144.053	40	830
	CFHT	0.171	1990 Sep. 09	8144.082	40	790
	CFHT	0.293	1991 Jan. 21	8277.803	40	680
	CFHT	0.304	1991 Jan. 21	8277.832	40	800
	CFHT	0.624	1991 Jan. 22	8278.744	40	940
	CFHT	0.635	1991 Jan. 22	8278.773	40	840
	CFHT	0.971	1991 Jan. 23	8279.726	40	760
	CFHT	0.981	1991 Jan. 23	8279.755	40	720
	CFHT	0.991	1991 Jan. 23	8279.783	40	730
	CFHT	0.675	1991 Jan. 25	8281.726	40	600
	CFHT	0.685	1991 Jan. 25	8281.754	40	800
	CFHT	0.696	1991 Jan. 25	8281.783	40	810
σ^2 CrB	CFHT	0.182	1990 Apr. 09	7991.001	60	1040
	CFHT	0.229	1990 Apr. 09	7991.054	60	1020
	CFHT	0.272	1990 Apr. 09	7991.103	60	980
	CFHT	0.607	1990 Sep. 06	8140.798	40	860
	CFHT	0.430	1990 Sep. 07	8141.736	40	1010
	CFHT	0.305	1990 Sep. 08	8142.733	40	1120
	CFHT	0.178	1990 Sep. 09	8143.728	40	1250
	CFHT	0.100	1991 Jan. 21	8278.135	40	1150
	CFHT	0.123	1991 Jan. 21	8278.161	30	920
	CFHT	0.973	1991 Jan. 22	8279.129	40	1000
	CFHT	0.998	1991 Jan. 22	8279.158	40	1070
	CFHT	0.845	1991 Jan. 23	8280.123	40	880
	CFHT	0.870	1991 Jan. 23	8280.152	40	910
	CFHT	0.597	1991 Jan. 25	8282.120	40	610
	CFHT	0.623	1991 Jan. 25	8282.150	40	610
II Peg	CFHT	0.040	1990 Sep. 06	8140.888	150	660
	CFHT	0.197	1990 Sep. 07	8141.876	160	670
	CFHT	0.334	1990 Sep. 08	8142.864	160	780
	CFHT	0.479	1990 Sep. 09	8143.840	160	600

Table 1 (continued)

System	Site	Rot. phase	Date	JD (2 440 000 +)	Exp. time (min)	S/N (pxl^{-1})
UX Ari	CFHT	0.781	1990 Sep. 06	8141.117	80	980
	CFHT	0.915	1990 Sep. 07	8141.976	80	810
	CFHT	0.067	1990 Sep. 08	8142.959	80	950
	CFHT	0.219	1990 Sep. 09	8143.933	80	820
	CFHT	0.023	1991 Jan. 21	8277.869	40	600
	CFHT	0.170	1991 Jan. 22	8278.816	60	800
	CFHT	0.326	1991 Jan. 23	8279.823	50	690
	CFHT	0.637	1991 Jan. 25	8281.822	50	710
EI Eri	CFHT	0.162	1990 Sep. 08	8143.134	50	470
	CFHT	0.671	1990 Sep. 09	8144.126	80	600
AR Lac	CFHT	0.231	1990 Sep. 07	8141.787	60	1050
	CFHT	0.731	1990 Sep. 08	8142.778	60	940
V824 Ara	AAT	0.229	1989 Aug. 17	7755.959	40	380
	AAT	0.247	1989 Aug. 17	7755.990	40	350
	AAT	0.847	1989 Aug. 18	7756.998	40	360
	AAT	0.865	1989 Aug. 18	7757.028	40	340
	AAT	0.882	1989 Aug. 18	7757.058	40	290
	AAT	0.900	1989 Aug. 18	7757.088	40	280
SZ Psc	AAT	0.611	1989 Aug. 17	7756.052	80	330
	AAT	0.624	1989 Aug. 17	7756.141	120	530
GX Lib	AAT	0.544	1989 Aug. 18	7756.913	160	560

configuration. With a thick GEC CCD (22 μm square pixels), the spectral resolution achieved is 37 000 (1.6 pxl). The medium quality atmospheric conditions being partly compensated by the high efficiency of the spectrograph, we typically obtain $S/N \approx 500\ pxl^{-1}$ in a 40 min exposure on a $V = 5.7$ mag star. At the CFHT, we use the $830\ gr\,mm^{-1}$ grating of the Coudé Spectrograph in second order, yielding a spectral resolution of 61 000 (2.6 pxl) when coupled to a RCA CCD (15 μm square pixels). With good seeing, we commonly obtain $S/N \approx 900\ pxl^{-1}$ on the same object and in the same exposure time.

3. Application to RS CVn systems

Seventy-six Stokes V spectra (Table 1) were recorded for 9 different RS CVn systems. Though these systems include at least two stars, some of those observed have a single-lined spectrum. Moreover, some of the visible stars are rotating too slowly for ZDI (i.e. $v \sin i < 20\ km\,s^{-1}$); the total sample studied in this paper therefore reduces to 12 stars (see Table 2).

3.1. Data analysis

To assess the statistical significance of any possible magnetic signature in the data, it is necessary to avoid all operations which may introduce additional uncertainty in the results. Hence, we only used averaging procedures (see next paragraph) to reduce photon noise as much as possible. A statistical test is then applied to the data to check whether the distortions of the circularly polarized spectra are significant, given the amplitude of the photon noise. We can then estimate safely if the field has been detected. No information other than a "detection probability" is derived about the field structure; local field strengths and filling factors are not computed since they require some modelling assumptions beyond the scope of this study. Moreover, in the context of complex magnetic topologies such as those expected for cool stars, effective field values have little meaning and are not listed here (except when compared to previously published values). Forthcoming papers will be devoted to maximum entropy image reconstructions from the polarized spectra presented below.

Consider now a Stokes V stellar spectrum obtained by the procedure mentioned in Sect. 2 and showing the three magnetically sensitive Fe I lines listed in Table 3. Since these lines are formed in almost identical conditions and have approximately the same Landé factor and equivalent width, we derive a composite Stokes V profile by simply averaging the circularly polarized signals associated with the individual lines. Firstly, this procedure has the obvious advantage of statistically reducing photon noise by 42%. Secondly, it lowers by a factor of 3 all possible errors caused by line blending; in particular, it ensures that the distortions generated in the composite Stokes V profile by the major blending contributor (Mn I 5505.87 Å line) will not exceed 14% of the main polarized signal due to the Fe I lines. When a given system was observed several times consecutively, the corresponding composite Stokes V profiles were also averaged (with an adequate recentring of the individual spectra to compensate for stellar motions) to increase the final S/N ratio. After such operations, the complete data set reduces to 56

Table 2. System stars studied. Column 4 indicates whether the system is a single- (SB1), double- (SB2) or triple (SB3) lined system. Column 5 and the followings list the system components (and some of their physical characteristics) that are studied in the present paper (from Strassmeier et al. 1988 except when indicated)

System	HD number	m_V (mag)	Binary nature	Star studied	Spectral type	$v \sin i$ ($\mathrm{km\,s^{-1}}$)	Orb. period (d)
UX Ari	21242	6.5	SB3[a]	Cool/	K0IV/	37/	6.43791
HR 1099	22468	5.7	SB2	Cool/	K1IV/	38/	2.83774
EI Eri	26337	6.95	SB1		G5IV	50	1.94722
GX Lib	136905	7.31	SB1		K1III	32	11.1345
σ^2 CrB	146361	5.7	SB2	Cool/hot	G0V/F6V	25/26	1.1397912
V824 Ara	155555	6.72	SB2	Cool/hot	K0IV/G5IV	30/34[b]	1.681652[c]
AR Lac	210334	6.09	SB2	Cool/hot	K0IV/G2IV	72/39	1.98322195
SZ Psc	219113	7.2	SB2	Cool/	K1IV/	65/	3.9658663
II Peg	224085	7.2	SB1		K2IV	21	6.724183

[a]Vogt & Hatzes (1991)
[b]This paper.
[c]Pasquini et al. (1991).

Table 3. Magnetically sensitive Fe I lines used in the analysis

Wavelength (Å)	Element	Effective Landé factor
5497.52	Fe I (15)	2.250
5501.47	Fe I (15)	1.875
5506.78	Fe I (15)	2.000

composite Stokes V profiles (10, 8 and 1 respectively for the cooler star of HR 1099, UX Ari and SZ Psc; 11, 2 and 2 respectively for each star of σ^2 CrB, AR Lac and V824 Ara; 4, 2 and 1 respectively for the visible star of II Peg, EI Eri and GX Lib). Information about them is given in Table 4.

To provide an objective criterion for deciding whether a magnetic field is detected on a star, we use the Chi-Square Probability Function (Abramowitz & Stegun 1965). For a star at a given phase, we calculate the χ^2 test statistics given by

$$\chi^2 = \frac{1}{n}\sum_{i=1}^{n}\left[\frac{V(\lambda_i)}{\sigma_i}\right]^2,$$

where λ_i ($i \in \{1,n\}$) denote the wavelengths at which the composite Stokes V profile is measured, and σ_i the corresponding error bars. This test quantifies how much the circularly polarized data deviate from a flat profile (no magnetic field) in units of the mean variance; in particular, it should be about 1.0 if nothing is detected on the star. The Chi-Square Probability Function $p(\chi^2|\nu)$, equal to:

$$p(\chi^2 \mid \nu) = P\left(\frac{\nu}{2}, \frac{\nu\chi^2}{2}\right)$$

(where P notes the Incomplete Gamma Function and ν the number of resolved elements in the observed spectrum), gives the probability that the model $V(\lambda)=0$ (no magnetic field) cannot account for the observed χ^2, i.e. that some magnetic field is detected on the star at this epoch. We consider that magnetic features are detected on the star if this probability is larger than 0.99, that there is marginal evidence that some field is present on the star if this probability ranges from 0.95 to 0.99, and that no magnetic field is detected at the observed phase if this probability is smaller than 0.95. Table 4 lists the derived χ^2 and detection probabilities for all 56 composite Stokes V profiles of the 12 observed stars.

3.2. *HR 1099*

HR 1099 = V711 Tau (K1IV + G5V) is a non-eclipsing, double-lined spectroscopic binary originally classified as an RS CVn type system by Bopp & Fekel (1976). Its brightness as well as its intense activity has made it one of the most observed stars for studying the so-called solar-stellar connection. On the photosphere of the K1 subgiant, huge moving dark spots are observed (Hall 1972; Dorren et al. 1981; Fekel 1983; Vogt 1988). Spectral signatures (e.g. Ca II H&K and Hα) indicate the presence of a high-temperature chromosphere (Bopp & Fekel 1976; Gondoin 1986). Strong X-ray (Walter et al. 1980) and radio (Owen et al. 1976) emissions are measured and interpreted as non-thermal radiations from the corona. As in all other program systems, tidal effects are strong enough in HR 1099 to almost synchronize the two stellar components.

ZDI is the first method to have succeeded in detecting directly magnetic fields at the surface of the K1 subgiant of HR 1099 (Donati et al. 1990a). During the two allocated nights at the AAT in Aug. 1989, 4 spectra were recorded around phase 0.513 and 6 spectra around phase 0.855 [in Fekel's ephemeris HJD $= 2\,442\,766.080 + 2.83774\phi$ where phase 0.0 refers to the first conjunction with the K1 subgiant in front (Fekel 1983)]. To compensate for the K1 subgiant motion from one exposure to another, we recentred the individual polarized spectra before averaging them. The resulting two composite Stokes V profiles at phases 0.513 and 0.855 are shown in Fig. 2a. At phase 0.855, the χ^2 is very high (actually the highest of the 56 composite Stokes V

Table 4. Statistical significance of the distortions observed in the composite Stokes V profiles. In the fifth column, probabilities written in bold style indicate a field detection

System	Date	Mean phase	Phases averaged	S/N in composite Stokes V profile	χ^2 (cool/hot)	Detec. prob. (coot/hot)
HR 1099	Aug. 1989	0.513	0.488, 0.511, 0.522, 0.530	2300	2.08/	**0.99**/
		0.855	0.829, 0.840, 0.850, 0.861, 0.871, 0.879	2150	11.29/	**1.00**/
	Sep. 1990	0.091	0.074, 0.085, 0.097, 0.107	2870	9.24/	**1.00**/
		0.155	0.136, 0.146, 0.161, 0.171	2840	3.43/	**1.00**/
		0.463	0.447, 0.457, 0.468, 0.479	3040	10.58/	**1.00**/
		0.808	0.793, 0.803, 0.813, 0.823	3310	3.20/	**1.00**/
	Jan. 1991	0.299	0.293, 0.304	1810	1.20/	0.75/
		0.630	0.624, 0.635	2190	1.85/	**0.99**/
		0.685	0.675, 0.685, 0.696	2220	2.80/	**1.00**/
		0.981	0.971, 0.981, 0.991	2210	4.92/	**1.00**/
σ^2 CrB	Apr. 1990	0.182	0.182	1810	2.56/1.09	**1.00**/0.65
		0.229	0.229	1760	1.75/0.94	0.98/0.47
		0.272	0.272	1700	2.22/0.63	**1.00**/0.12
	Sep. 1990	0.178	0.178	2170	3.15/0.69	**1.00**/0.18
		0.305	0.305	1940	5.62/1.25	**1.00**/0.79
		0.430	0.430	1760	1.45/1.42	0.90/0.89
		0.607	0.607	1490	0.92/0.82	0.45/0.33
	Jan. 1991	0.111	0.100, 0.123	2550	2.95/1.47	**1.00**/0.91
		0.610	0.597, 0.623	1500	1.27/0.50	0.80/0.04
		0.857	0.845, 0.870	2180	2.07/1.63	**0.99**/0.96
		0.985	0.973, 0.998	2530	2.01/1.06	**0.99**/0.61
II Peg	Sep. 1990	0.040	0.040	1150	5.68	**1.00**
		0.197	0.197	1170	5.25	**1.00**
		0.334	0.334	1360	5.24	**1.00**
		0.479	0.479	1040	7.50	**1.00**
UX Ari	Sep. 1990	0.067	0.067	1640	4.37/	**1.00**/
		0.219	0.219	1420	1.73/	0.97/
		0.781	0.781	1690	3.23/	**1.00**/
		0.915	0.915	1400	4.18/	**1.00**/
	Jan. 1991	0.023	0.023	1030	1.62/	0.95/
		0.170	0.170	1390	2.11/	**1.00**/
		0.326	0.326	1190	1.44/	0.90/
		0.637	0.637	1230	1.51/	0.92/
EI Eri	Sep. 1990	0.162	0.162	810	1.11	0.68
		0.671	0.671	1050	1.25	0.81
AR Lac	Sep. 1990	0.231	0.231	1820	1.00/1.07	0.55/0.63
		0.731	0.731	1630	0.74/0.76	0.19/0.21
V824 Ara	Aug. 1989	0.238	0.229, 0.247	890	1.02/0.91	0.57/0.46
		0.873	0.847, 0.865, 0.882, 0.900	1100	1.57/0.96	0.91/0.51
SZ Psc	Aug. 1989	0.618	0.611, 0.624	1080	0.95/	0.47/
GX Lib	Aug. 1989	0.544	0.544	960	1.03	0.58

profiles, see Table 4), reflecting the 14σ total amplitude of the detected Zeeman signature. It indicates undoubtedly the presence of a magnetic field. At phase 0.513, the Zeeman signature is smaller (6σ), but large enough to indicate a magnetic field ($p=0.99$). Due to its small amplitude, this magnetic signature was not considered in the preliminary modelling of Donati et al. (1990a). The rotational modulation of the polarized signature between the two phases is obvious.

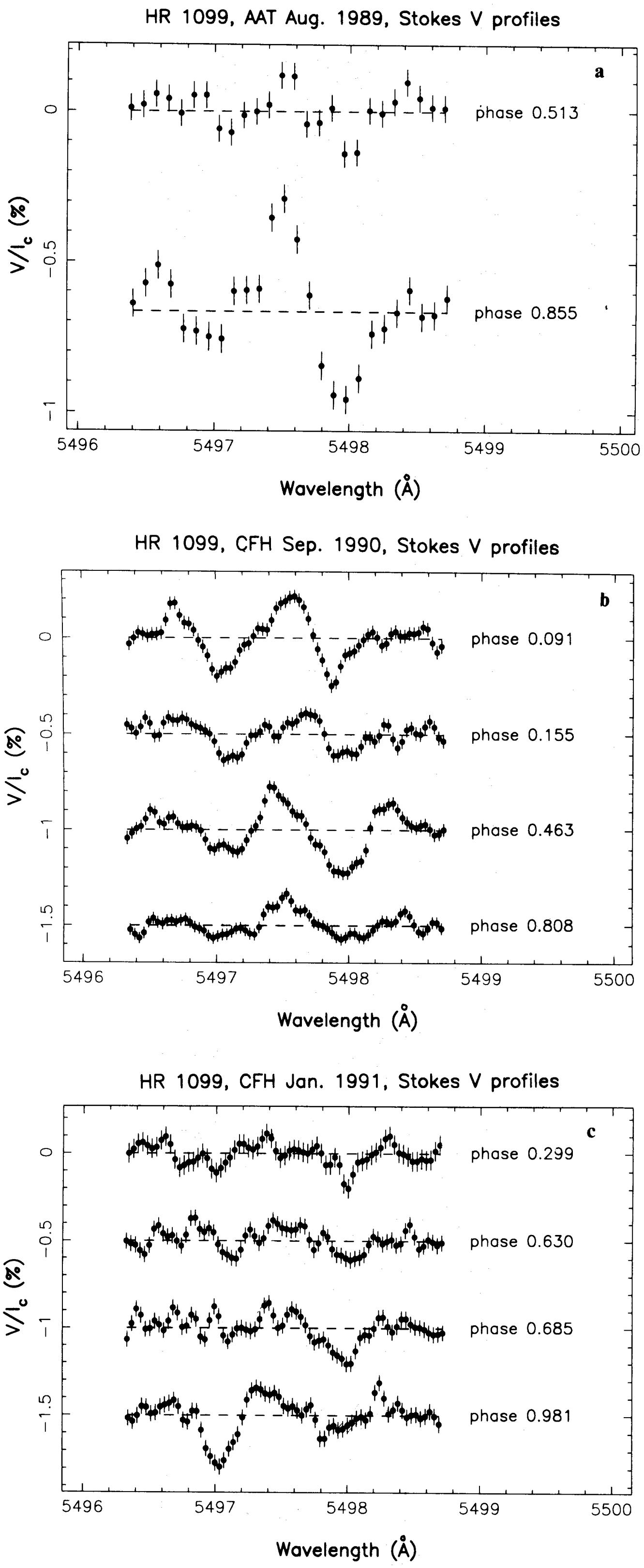

Fig. 2a–c. Composite Stokes V profiles for the cool star of HR 1099 derived from circularly polarized spectra recorded at the AAT in Aug. 1989 (**a**), and at the CFHT in Sep. 1990 (**b**) and in Jan. 1991 (**c**). Note that, as in all following graphs, these Stokes V profiles are the *average* of all three Fe I lines in Table 3, even though the wavelength axis refers only to the Fe I 5497.52 Å line

Twenty-six more Stokes V spectra of HR 1099 were collected in Sep. 1990 and Jan. 1991 at the CFHT, covering about 8 different rotational phases (0.091, 0.155, 0.463 and 0.808 in Sep. 1990; 0.299, 0.630, 0.685 and 0.981 in Jan. 1991). Recentring and averaging procedures on these spectra led to 8 composite Stokes V profiles of the K1 subgiant, shown in Fig. 2b, c. All of them show significant polarized distortions (see Table 4) except at phase 0.299 for which the larger photon noise error bars prevent us from detecting safely any magnetic field on HR 1099. Once more, the changes of the polarized signal with rotation are quite clear.

Looking now at *how* these composite Stokes V profiles are modulated by rotation gives us a good idea of the complexity of the magnetic distribution involved. Obviously, we are no longer in the classical Ap star situation with two polarities slowly alternating throughout the rotation cycle, but in a more unusual and tricky one where rotation generates rapid and apparently random changes from one phase to another. The composite Stokes V profiles often show several reversals (as in phase 0.091 and 0.463 for instance), which confirms the complexity of the magnetic distribution of HR 1099. This explains in particular why Brown & Landstreet (1981) obtained only a non significant effective field measurement (-58 ± 70 G). In fact, effective field values calculated from our circularly polarized spectra never exceed 50 G, except at phase 0.855 (AAT data) where it reaches 110 G.

Comparing Aug. 1989 (phases 0.513 and 0.855) and Sep. 1990 (phases 0.463 and 0.808) profiles, we notice a significant change in both Stokes V and I profiles, indicating a modification of the photospheric structure within a period of a year. It is more difficult to reach a conclusion about some possible variability between Sep. 1990 and Jan. 1991 since the star was not observed at the same rotational phase in both data sets.

The hotter G5 dwarf of HR 1099 is also chromospherically active (Bopp & Fekel 1976) though significantly less than the K1 subgiant (Buzasi et al. 1991). We find no circularly polarized signature associated with this component. However, since no spatial resolution may be achieved through ZDI on this slowly rotating star ($v \sin i = 13$ km s^{-1}), opposite magnetic polarities likely cancel each other's effect in the circularly polarized spectra.

3.3. σ^2 CrB

The system σ^2 CrB (G0V + F6V) is a double-lined spectroscopic binary for which Skillman & Hall (1978) observed light variations similar to those occurring in RS CVn type systems. Both stars of σ^2 CrB are chromospherically active dwarfs (Bopp 1984). Having approximately the same mass, radius, gravity and rotation rate (Barden 1985), their spectra are very similar. X-ray emission (Walter et al. 1980) also indicates the presence of coronal structures.

The system was first observed in Apr. 1990 at the CFHT at phase 0.182, 0.229 and 0.272 [in ephemeris HJD = 2 423 869.3925 + 1.1397912ϕ where phase 0.0 refers to the conjunction with the G0 dwarf in front (Bakos 1984)]. At each phase, one composite Stokes V profile was derived for each component (Figs. 3a and 4a). On the G0 dwarf, we can safely infer that some magnetic field is detected at phases 0.182 and 0.272 (see Table 4). Some distortions are also visible in the circularly polarized spectrum at phase 0.229. Even though they can not be interpreted as a definite detection from the lower χ^2, it is likely that they are caused by the

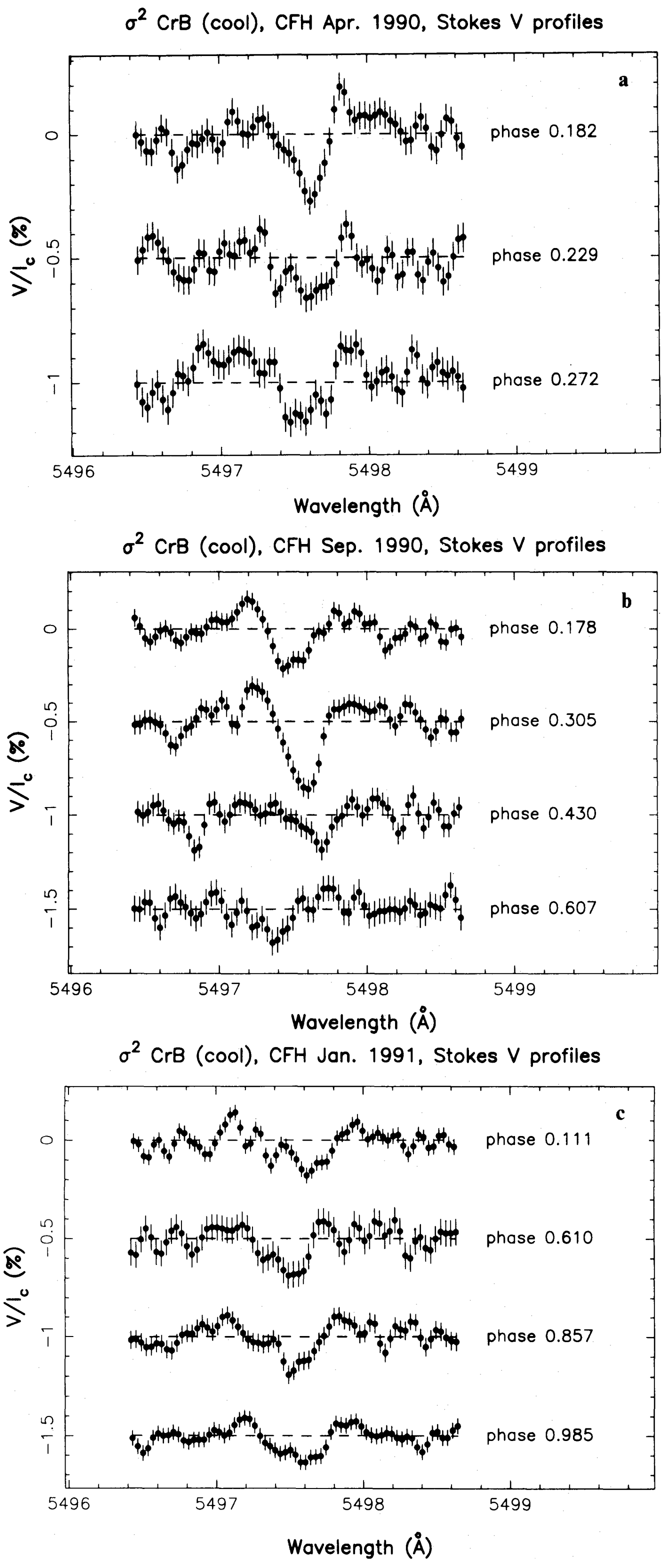

Fig. 3a–c. Composite Stokes V profiles for the cool star of σ^2 CrB derived from circularly polarized spectra recorded at the CFHT in Apr. 1990 (**a**) Sep. 1990 (**b**) and in Jan. 1991 (**c**)

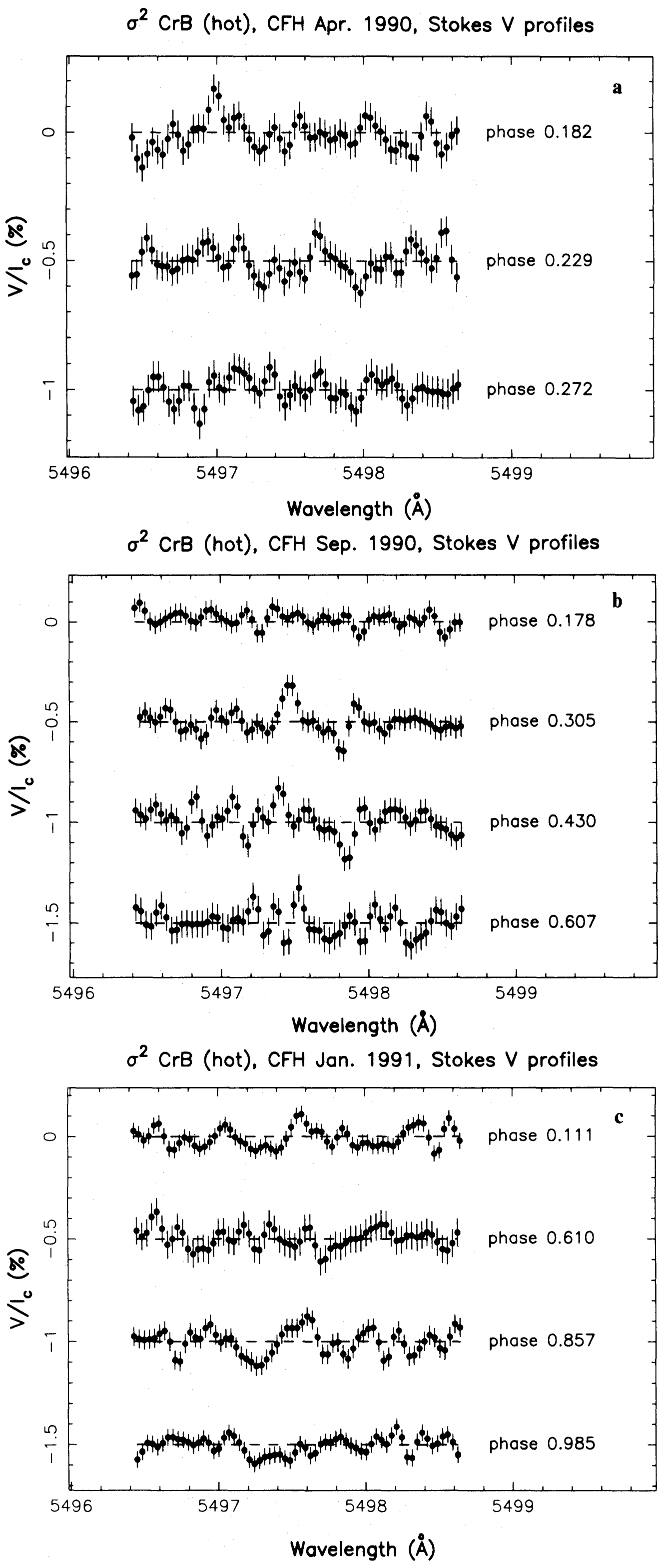

Fig. 4a–c. Same as Fig. 3 for the hot component of σ^2 CrB

magnetic features detected at phases 0.182 and 0.272. No field is detected on the hotter F6 companion.

More circularly polarized spectra were obtained at the CFHT in Sep. 1990 (4 spectra at phases 0.178, 0.305, 0.430 and 0.607) and Jan. 1991 (8 spectra around phases 0.111, 0.610, 0.857 and 0.985). Once more, one composite Stokes V was derived per mean phase and per star (Figs. 3b, c and 4b, c). For the G0 dwarf, 5 phases (out of 8) are associated with large χ^2 values (larger than 2.0, see Table

4) indicating an unambiguous detection of magnetic field. The distortions in the Stokes V profiles exhibit obvious changes with rotation, reaching a maximum amplitude of 0.6% of the unpolarized continuum level at phase 0.305. On the hotter F6 component, there is marginal evidence of magnetic field in the composite Stokes V spectrum at phase 0.857 ($p=0.96$). However, we do not yet regard this result as significant since no other magnetic evidence is found in the entire data set of the hotter star.

The shape of the Zeeman signatures witnesses the complexity of the magnetic distributions. The Zeeman signatures of the G0 dwarf, when detected, occur primarily in the central regions of the composite Stokes V profiles rather than in the wings. This suggests that the corresponding magnetic features could be located at high latitude (where rotational modulation is minimal). A complete 2D maximum entropy reconstruction of the field structure is needed to confirm this supposition. Since the difference between the composite Stokes V profile of the G0 dwarf at phase 0.182 (Apr. 1990) and that at phase 0.178 (Sep. 1990) exceeds the noise level, it is likely that the photospheric structure has changed within this period. Note, however, that the largest Zeeman signatures have been constantly observed around the first quadrature (phase 0.250), indicating that this photospheric variability is local rather than global.

3.4. II Peg

II Peg (K2IV) is a single-lined spectroscopic binary, classified as an RS CVn system by Vogt (1981a). Its huge photometric rotational modulation and its intrinsic variability was first discovered by Chugainov (1976) and tentatively interpreted with a cool spot model by Vogt (1981b) and, more recently, by Rodonò et al. (1986). II Peg is also very chromospherically active (Vogt 1981a), as well as being an intense radio (Spangler et al. 1977) and X-ray (Walter et al. 1980) source in a quasi-permanent flaring state.

Since II Peg was only visible in Sep. 1990 (CFHT run), half a rotation cycle [phases 0.040, 0.197, 0.334 and 0.479 in ephemeris HJD $=2\,443\,030.239+6.724183\phi$ (Rucinski 1977)] has been observed. Although one of the faintest program stars, all composite Stokes V profiles exhibit large distortions of the order of 1% of the unpolarized continuum level (see Fig. 5). Such signatures can be interpreted quite safely as magnetic ($\chi^2>5.0$), show complex shapes and obvious rotational modulation. This suggests that the high activity of II Peg is magnetically driven and makes it a preferred target for future observations.

A point to stress here is the poor significance of the effective field in the case of such complex magnetic topologies; though Zeeman signatures are obviously present in the Stokes V profiles of II Peg, the corresponding effective field values never exceed 70 G. The marginal value of -515 G obtained by Vogt (1980) on this star is therefore not supported by our new set of observations.

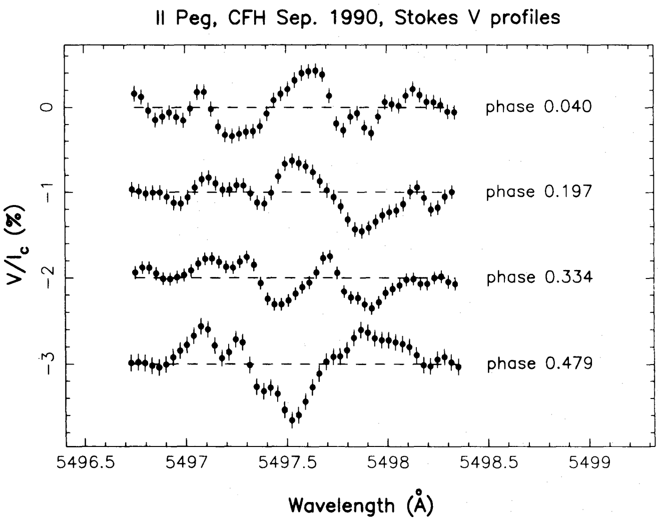

Fig. 5. Composite Stokes V profiles for II Peg derived from circularly polarized spectra recorded at the CFHT in Sep. 1990

3.5. UX Ari

UX Ari (K0IV + G5V) was first known as a double-lined spectroscopic binary, until Vogt & Hatzes (1991) discovered a third faint component, probably in a long period orbit about the central binary. The binary shows all kinds of activity signatures attributed mostly to the brighter K0 subgiant. Photometric variability or profile distortions (Vogt & Hatzes 1991), strong chromospheric emission in the Hα and Ca II lines, as well as radio and X-ray fluxes from coronal loops are detected throughout the whole spectrum (see Strassmeier et al. 1988 for details).

UX Ari was observed in both Sep. 1990 [phases 0.067, 0.219, 0.781 and 0.915 in ephemeris HJD $=2\,440\,133.766+6.43791\phi$ (Carlos & Popper 1971)] and Jan. 1991 (phases 0.023, 0.170, 0.326 and 0.637) CFHT runs. The corresponding composite Stokes V spectra of the K0 subgiant are displayed in Fig. 6a, b; large Zeeman signatures are obtained at 3 phases around phase 0.900 in September, establishing the presence of magnetic fields on its surface. In the Jan. 1991 data set, the field is only detected at phase 0.170. Even though distortions are also seen in the composite Stokes V profiles at other phases, higher noise levels preclude any definite conclusion about their possible magnetic origin (see Table 4).

This system was observed several times with conventional polarimetric methods (Brown & Landstreet 1981; Borra et al. 1984). Both studies involved the simultaneous use of hundreds of lines (340 and 1500 respectively) to allow magnetic measurements with very low error bars. However, no significant detection was obtained, the maximum strength measured being 84 ± 35 G. In fact, the effective field values derived from our composite Stokes V profiles do not exceed this value either, confirming that conventional Zeeman polarimetry is not adequate for cool solar-type stars with spotted magnetic topologies.

Vogt & Hatzes (1991) suggest that the photospheric structure varies on timescales of a few months. It is, however, difficult to confirm this result from our magnetic data; even though the star was observed in about the same configuration in Sep. 1990 (phase 0.067) and Jan. 1991 (phase 0.023), the corresponding circularly polarized spectra are in agreement within the noise level.

As in HR 1099, no field is detected on the secondary star, the $v\sin i$ of which is too low (6 km s^{-1}) for ZDI.

3.6. EI Eri and AR Lac

EI Eri (G5IV) is a single-lined spectroscopic binary, classified as an RS CVn system from its photospheric variability by Fekel et al. (1982). In addition to its Ca II and strong ultraviolet emission lines typical of chromospherically active stars, the star emits at radio frequencies, but no X-ray measurement is available yet (see

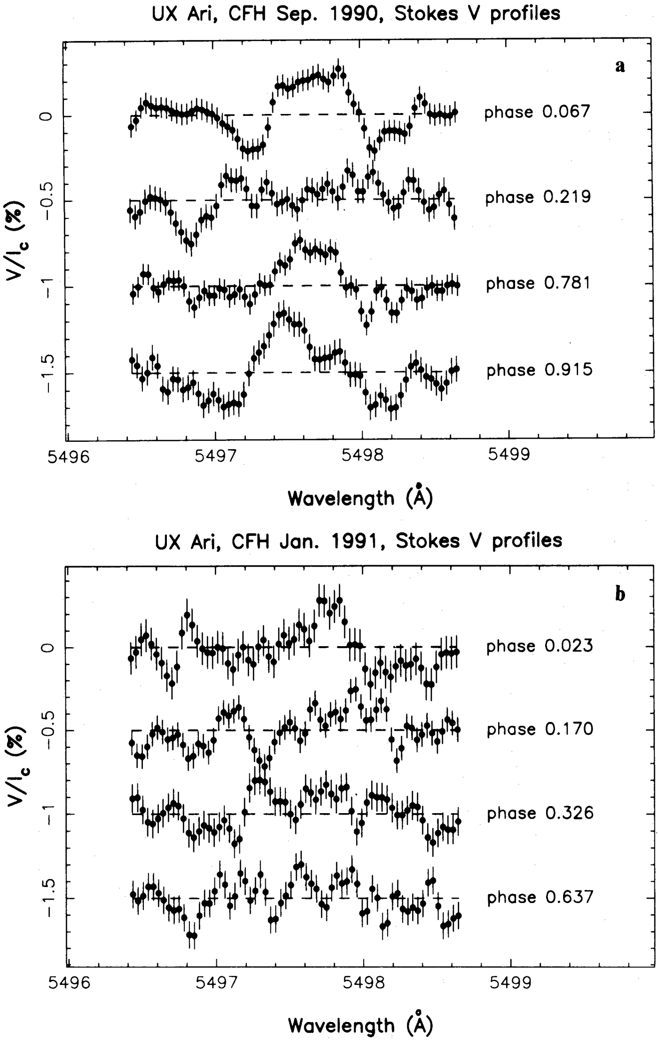

Fig. 6a and b. Composite Stokes V profiles for the cool star of the central binary system of UX Ari derived from circularly polarized spectra recorded at the CFHT in Sep. 1990 (**a**) and in Jan. 1991 (**b**)

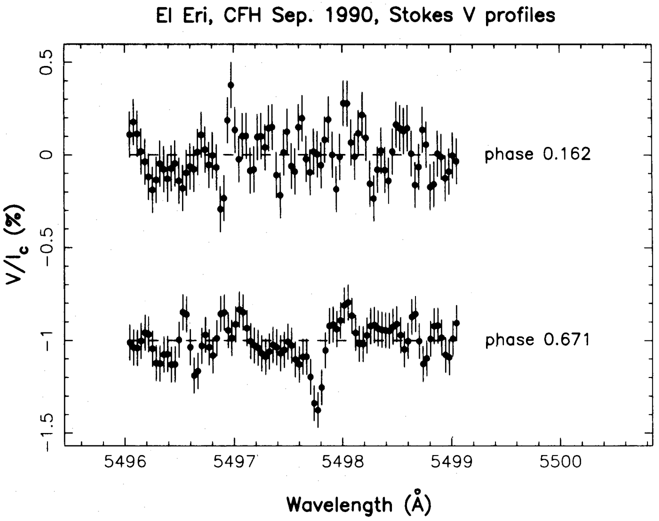

Fig. 7. Composite Stokes V profiles for EI Eri derived from circularly polarized spectra recorded at the CFHT in Sep. 1990

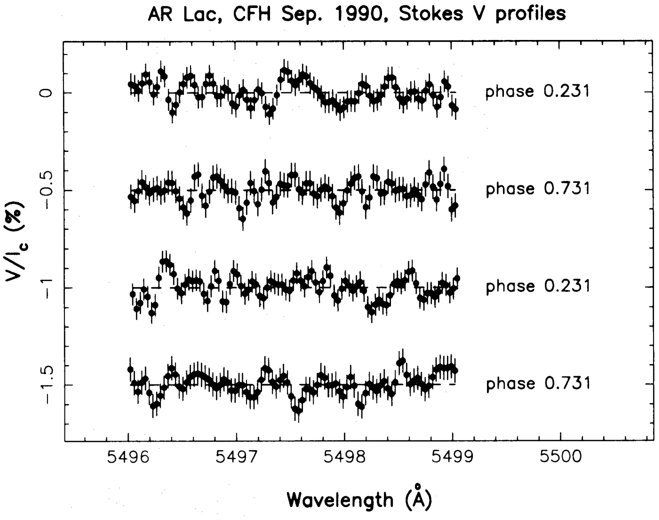

Fig. 8. Composite Stokes V profiles for the cool (2 upper curves) and the hot (2 lower curves) of AR Lac, derived from circularly polarized spectra recorded at the CFHT in Sep. 1990

Strassmeier et al. 1988). This star has been the subject of several recent stellar imaging studies (Strassmeier et al. 1991). AR Lac (K0IV + G2IV) is a double-lined eclipsing spectroscopic binary, both components of which exhibiting all classical signatures of stellar activity (Strassmeier et al. 1988). Since eclipses in this system are total, it is an obvious target for imaging atmospheric structures (Neff et al. 1989).

Both stars were observed during the Sep. 1990 CFHT run. Since their orbital period is close to two days [1.947 d for EI Eri (Fekel et al. 1987) and 1.983 d for AR Lac (Hall & Kreiner 1980)], they have been only observed twice non redundantly, at phases 0.162 and 0.671 for EI Eri (in Fekel et al. 1987 ephemeris HJD $= 2\,446\,074.871 + 1.94722\phi$) and at phases 0.231 and 0.731 for AR Lac (in Hall & Kreiner 1980 ephemeris HJD $= 2\,426\,624.3628 + 1.98322195\phi$).

For EI Eri, the relative faintness of the star is responsible for the large error bars precluding any magnetic detections at either observed phases, as shown in Fig. 7 and Table 4. In the case of AR Lac, composite Stokes V spectra were derived for both cool (Fig. 8, two upper curves) and hot (two lower curves) components. No detection is obtained for either stars at both phases, though the error bars are relatively small. However, due to the very poor phase coverage achieved, no conclusion can be inferred yet about the magnetic structures of these stars.

3.7. *V824 Ara, SZ Psc and GX Lib*

Snapshots of these three RS CVn systems were obtained in the Aug. 1989 AAT run. V824 Ara (K0IV + G5IV) and SZ Psc (K1IV + F8V) are double-lined spectroscopic binaries, very closely interacting. According to Hall & Kreiner (1980), mass transfer between both components of SZ Psc has already begun, given the constant decrease with time of its orbital period for the last 60 yr. GX Lib (K1III) is a single-lined spectroscopic binary. All of them are chromospherically active (Strassmeier et al. 1988) and show unpolarized profile distortions indicating the presence of temperature inhomogeneities (Kürster 1992; Vogt & Penrod 1983; Dempsey et al. 1992).

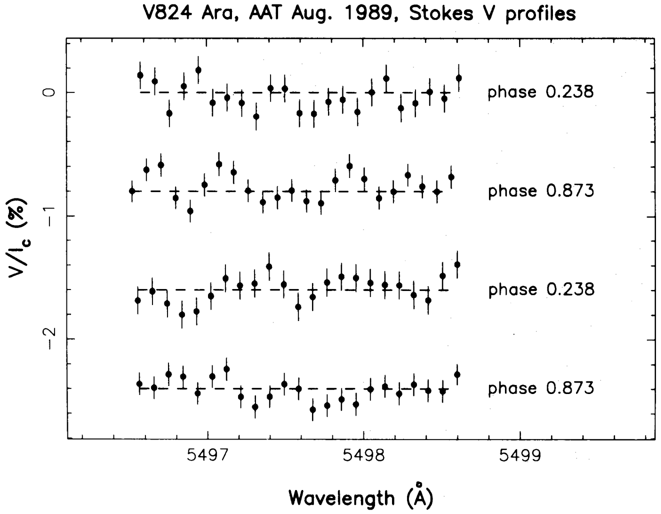

Fig. 9. Composite Stokes V profiles for the cool (2 upper curves) and the hot (2 lower curves) of V824 Ara, derived from circularly polarized spectra recorded at the AAT in Aug. 1989

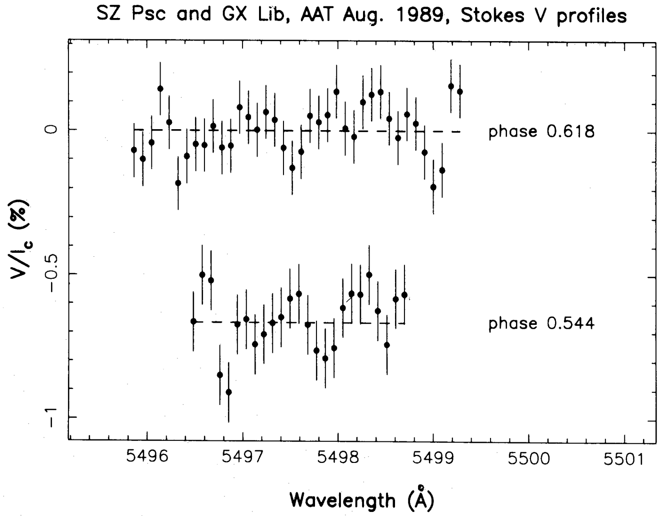

Fig. 10. Composite Stokes V profiles for the cool star of SZ Psc (upper curve) and for GX Lib (lower curve), derived from circularly polarized spectra recorded at the AAT in Aug. 1989

Comparing the spectral line width of both components of V824 Ara with those of other stars with known $v \sin i$, we derive values of $v \sin i$ for the cool and hot stars, respectively equal to 30 ± 2 and 34 ± 2 km s^{-1}. These values are in reasonable agreement with the less accurate new ones obtained by Pasquini et al. (1991) from CORAVEL data (29 ± 5 and 37 ± 3 km s^{-1}). Incorporating previous radial velocity measurements by Benett et al. (1962) with their own ones, Pasquini et al. (1991) also derived a new ephemeris for V824 Ara (HJD $= 2\,446\,998.8306 + 1.681652\phi$ where phase 0.0 refers to the conjunction with the K0 subgiant in front). Our observations then correspond to the average orbital phases 0.238 and 0.873, in good agreement with the radial velocities measured for both stellar components. After recentring and averaging the polarized spectra obtained around these two phases, two composite Stokes V spectra are derived for each component (Fig. 9). No evidence of magnetic field is obtained, as noted in Table 4.

As the period and therefore the time of first conjunction of SZ Psc vary with time, we cannot use the published ephemeris of Hall & Kreiner (1980) to derive orbital phases. However, assuming that the orbital elements given by Jakate et al. (1976) still apply, we can match uniquely the observed radial velocities of both components if the orbital phases of the two spectra are set to 0.611 and 0.624 (where phase 0.0 refers to the conjunction with the K1 subgiant in front). This correction corresponds to an increase of 0.452 d (0.114 cycle) of Hall & Kreiner's (1980) epoch of first conjunction, in agreement with the steady decrease of the orbital period observed for this system. The derived composite Stokes V profiles of the K1 subgiant at the observed mean phase (0.618) shows no obvious Zeeman signature (see upper spectrum of Fig. 10). As in HR 1099 and UX Ari, the hotter (F8V) component has too low a $v \sin i$ for ZDI.

The lower part of Fig. 10 shows the composite Stokes V profile obtained for GX Lib (observed at phase 0.544). No distortions of magnetic origin can be reliably identified.

However, as for EI Eri and AR Lac, no conclusions can be derived about the magnetic structures of these stars since they have not been observed throughout a complete rotation cycle.

4. Discussion

In contrast to the general trend over the last decade, we have revived the use of circular polarization in the domain of magnetic field measurements on cool stars. With ZDI, we recorded Stokes V profiles of magnetically sensitive lines for a set of 9 very active bright RS CVn systems. Definite evidence for magnetic fields has been obtained for 4 of them, namely HR 1099, σ^2 CrB, UX Ari and II Peg. With the previous papers (Donati et al. 1990a; Donati 1990), this work represents the first successful attempt to detect directly magnetic fields on RS CVn systems, if we exclude the much debated and discrepant result on λ And (Marcy & Bruning 1984; Giampapa et al. 1983; Gondoin et al. 1985). From these first results, what conclusions can we derive about the ability of ZDI to detect magnetic fields of rapidly rotating stars on one hand, and about activity of RS CVn systems on the other?

Let us first divide the 12 observed stars into 2 subsets. The first contains stars in which the field *has been* detected at least once, and the second includes all others (on which no field was seen). Among subset 1, the field was detected in 75% of the recorded spectra; Zeeman signatures have indeed been identified at 4 different phases out of 4 observed on II Peg, at 9 different phases out of 10 observed on the K1 subgiant of HR 1099, at 7 different phases out of 11 observed on the G0 dwarf of σ^2 CrB and at 4 different phases out of 8 observed on the K0 subgiant of UX Ari. In subset 2, we find some stars on which the field was repeatedly *not* detected. For instance, no evidence of Zeeman signatures are observed in all 11 polarized profiles recorded for the F6 dwarf of σ^2 CrB and in the two profiles obtained for both stars of AR Lac, although a relative noise as low as 0.07% was achieved. Being more than an arbitrary partition of the program stars, these two subsets have therefore real meaning and contain respectively stars on which ZDI is very efficient in detecting magnetic fields (subset 1), and stars on which ZDI has been totally inefficient to date (subset 2). Even more striking is the particular case of σ^2 CrB for which each component belongs to a different subset, though physically very similar. What physical property is then hidden behind the way ZDI differentiates stars?

Technical reasons may be invoked. As studied in Donati et al. (1989), a large $v \sin i$ may help, on one hand, to disclose spectroscopically opposite polarities in small magnetic groups, resulting in enhancing the polarized magnetic signature in the measured Stokes V profile. On the other hand, a large $v \sin i$ spreads spectral lines and Zeeman signatures on a wider wavelength interval, making both Stokes I and V shallower. The latter effect may be partly responsible for the fact that all three (out of 12) program stars with $v \sin i$ larger than 50 km s^{-1} show *no* Zeeman signature. This does not, however, account for the non detection on the hotter component of σ^2 CrB or on that of AR Lac, which both have $v \sin i < 40$ km s^{-1} (see Table 2).

This dual behaviour of ZDI probably reflects differences in stellar atmospheres. As a rule, magnetic field is detected with ZDI if the spacing between features of opposite polarity is larger than the resolution of the imaging process, i.e. than the width of the intrinsic stellar profile broadened by macroturbulence. As mentioned above, the circularly polarized signatures presented in this paper are always much more complex than in the simple Ap star dipole case (e.g. Donati & Semel 1990), indicating highly multipolar structures on the observed stars. However, even if more complex than a dipole, the topologies generating the observed Zeeman signatures probably include monopolar features covering at least several percent of the stellar surface (Donati et al. 1990a), making their detection possible. By contrast, stars on which the field is repeatedly not detected must possess, if magnetic, small monopolar regions associated in close multipolar groups and cancelling their mutual effect in the Stokes V profiles.

Hence, subset 1 contains stars with large monopolar magnetic regions. Moreover, the magnetic flux of these stars is sufficiently strong to produce statistically observable Zeeman signatures in about 75% of the rotation cycle. Note however that we still have to establish that their activity is due to the magnetic field itself, i.e. that the observed magnetic regions coincide with the photospheric temperature inhomogeneities and chromospheric plages. As 2D stellar surface maps are needed to answer this question, the way is left open for further interpretations of the present data with a maximum entropy image reconstruction code (Brown et al. 1991). Concerning stars of subset 2, we can say only that magnetic features on their surface (if any) are much smaller than those of stars in subset 1. We conclude that different magnetic structures (having at least different horizontal size scales) are observed on different stars. Most striking is that even stars physically very similar, such as both components of σ^2 CrB, may show these differences in magnetic structures.

What processes could cause the difference in size of stellar magnetic regions? Using σ^2 CrB may be fruitful as both components, though almost identical, have different sizes of magnetic regions. Since this system is a double-lined spectroscopic binary, radii, masses and rotation rates of both components are well determined, and found to be equal within the uncertainties (Barden 1985). In fact, these two components differ mainly by $\approx$400 K in effective temperature. Although small, this difference is sufficient for each star of the system to be located on either side of the steep deepening of the convection zone with decreasing effective temperatures. This suggests that different convective depths generate magnetic regions of different size. Since convective cells are probably larger than the magnetic flux ropes they confine, the depth of the convection zone may be a rough upper limit for the size of the magnetic regions. Such an argument could explain qualitatively why large magnetic regions such as those detected of the G0 dwarf of σ^2 CrB are not observed on the F6 dwarf of the same system. Alternatively, it may be that the two stars are not in the same phase of their magnetic cycle; from a low multipole field structure, mainly radial and poloidal (at the activity minimum), the topology could become progressively more complex with smaller monopolar regions as differential rotation progressively winds the field lines around the star.

Obviously, a better understanding of these mechanisms will be obtained when 2D magnetic images corresponding to the Stokes V spectra presented herein are available. A maximum entropy image reconstruction code (Brown et al. 1991) is currently being used for this purpose. Additional observations will then allow us to follow the distortions of magnetic topologies along activity cycles.

Acknowledgements. This work has been supported by the Natural Science and Engineering Research Council of Canada. We are grateful to S. Vogt (as the referee), F. Praderie and D. Gray for valuable comments about the manuscript, to J. Glaspey, K. Taylor, P. Gillingham and all members of the CFHT and AAT staff for their help with instrumental settings, and to C. Catala, T. Ducros and Li Jing for their active involvement in data collection. We especially thank O. Durand for his important role in building the polarimeter used at the CFHT, without which most of this study could not have been done. We acknowledge the University of Sydney, the Australian Research Council, the Institut National des Sciences de l'Univers and the French Ministry of Foreign Affairs for travel funds.

References

Abramowitz M., Stegun I.A., 1965, Handbook of Mathematical Functions. Dover, New York
Babcock H.W., 1958, ApJS 3, 141
Bakos G.A., 1984, AJ 89, 1740
Barden S.C., 1985, ApJ 295, 162
Benett W.W., Evans D.S., Laing J.D., 1962, Roy. Obs. Bull. n° 61
Bopp B.W., 1984, ApJS 54, 387
Borra E.F., Edwards G., Mayor M., 1984, ApJ 284, 211
Bopp B.W., Fekel F.C., 1976, AJ 81, 771
Brown D.N., Landstreet J.D., 1981, ApJ 246, 899
Brown S.F., Donati J.-F., Rees D.E., Semel M., 1991, A&A 250, 463
Buzasi D., Huenemoerder D.P., Ramsey L.W., 1991, PASP 103, 1077
Carlos R.C., Popper D.M., 1971, PASP 83, 504
Chugainov P.F., 1976, Izv. Krymskoj Astrofiz. Obs. 54, 89
Dempsey R.C., Bopp B.W., Strassmeier K.G., et al., 1992, ApJ 392, 187
Donati J.-F., 1990, PhD Thesis, Université Paris VII, Paris
Donati J.-F., Semel M., 1990, Sol. Phys. 128, 227
Donati J.-F., Semel M., Praderie F., 1989, A&A 225, 467
Donati J-F., Semel M., Rees D.E., Taylor K., Robinson R.D., 1990a, A&A 232, L1
Donati J.-F., Semel M., del Toro Iniesta J.C., 1990b, A&A 233, L17
Dorren J.D., Siah M.J., Guinan E.F., McCook G.P., 1981, AJ 86, 572
Fekel F.C., 1983, ApJ 268, 274
Fekel F.C., Hall D.S., Henry G.W., Landis H.J., Renner T.R., 1982, Inf. Bull. Var. Stars n° 2110

Fekel F.C., Quigley R., Gillies K., Africano J.L., 1987, AJ 94, 726

Giampapa M.S., Golub L., Worden S.P., 1983, ApJ 268, L121

Gondoin Ph., 1986, A&A 160, 73

Gondoin Ph., Giampapa M.S., Bookbinder J.A., 1985, ApJ 297, 710

Gray D.F., 1988, Lectures on Spectral-Line Analysis: F, G and K stars. The Publisher, Arva

Hall D.S., 1972, PASP 84, 323

Hall D.S., Kreiner J.M., 1980, Acta Astron. 30, 387

Jakate S., Bakos G.A., Fernie J.D., Heard J.F., 1976, AJ 81, 250

Kürster M., 1992, in : Giampapa M.S., Bookbinder J.A. (eds.) Seventh Cambridge Workshop on Cool Stars, Stellar Systems, and the Sun. ASP Conf. Ser. Vol. 26, p. 249

Marcy G.W., Bruning D.H., 1984, ApJ 281, 286

Neff J.E., Walter F.M., Rodonò M., Linsky J.L., 1989, A&A 215, 79

Owen F.N., Jones T.W., Gibson D.M., 1976, ApJ 210, L27

Pasquini L., Cutispoto G., Gratton R., Mayor M., 1991, A&A 248, 72

Piskunov N.E., Tuominen I., Vilhu O., 1990, A&A 230, 363

Preston G.W., 1971, ApJ 164, 309

Rice J.B., Wehlau W.H., 1990, A&A 233, 503

Robinson R.D., 1980, ApJ 239, 961

Rodonò M., Cutispoto G., Pazzani V., et al., 1986, A&A 165, 135

Rucinski S.M., 1977, PASP 89, 280

Saar S.H., 1988, ApJ 324, 441

Saar S.H., 1990, in: Stenflo J.O. (ed.) Proc. IAU Symp. 138, Solar Photosphere: Structure, Convection and Magnetic Fields. Kluwer, Dordrecht, p. 427

Saar S.H., 1991, in: Tuominen I., Moss D., Rüdiger G. (eds.) Proc. IAU Coll. 130, The Sun and Cool Stars: Activity, Magnetism, Dynamos. Springer, Berlin, p. 389

Semel M., 1987, A&A 178, 257

Semel M., 1989, A&A 225, 456

Semel M., Donati J.-F., Rees D.E., 1992, A&A (submitted)

Skillman D.R., Hall D.S., 1978, Inf. Bull. Var. Stars n° 1529

Spangler S.R., Owen F.N., Hulse R.A., 1977, AJ 82, 989

Strassmeier K.G., Fekel F.C., Bopp B.W., Dempsey R.C., Henry G.W., 1990, ApJS 72, 191

Strassmeier K.G., Hall D.S., Zeilik M., et al., 1988, A&AS 72, 291

Strassmeier K.G., Rice J.B., Wehlau W.H., et al., 1991, A&A 247, 130

Vogt S.S., 1980, ApJ 240, 567

Vogt S.S., 1981a, ApJ 247, 975

Vogt S.S., 1981b, ApJ 250, 327

Vogt S.S., 1988, in: Cayrel de Strobel G., Spite M. (eds.) Proc. IAU Symp. 132, The Impact of Very High S/N Spectroscopy on Stellar Physics. Kluwer, Dordrecht, p. 253

Vogt S.S., Hatzes A.P., 1991, in: Tuominen I., Moss D., Rüdiger G. (eds.) Proc. IAU Coll. 130, The Sun and Cool Stars: Activity, Magnetism, Dynamos. Springer, Berlin, p. 297

Vogt S.S., Penrod G.D., 1983, PASP 95, 565

Walter F.M., Cash W., Charles P.A., Bowyer C.S., 1980, ApJ 236, 212

Zahn J.-P., 1977, A&A 57, 383